ESA STUDY CONTRACT REPORT

Deliverable 4 under WP2: Report on derivation of satellite based vegetation metrics and downscaling to high-resolution data

ESA Contract No: 4000117034/16/NL/NDe	SUBJECT: **SURGE**: Simulating the cooling effect of urban greenery based on solar radiation modelling and a new generation of ESA sensors	CONTRACTOR: Pavol Jozef Šafárik University in Košice, Institute of Geography
* ESA CR( )No:	No. of Volumes:. 1 This is Volume No: 1.0	CONTRACTOR'S REFERENCE:

ABSTRACT:

Urban greenery in moderate climate zones contains many deciduous plant species with leaf-on and leaf-off periods that affect the solar radiation transmittance and thus the cooling effects of greenery in the city which is combined with the more pronounced effect of the solar incidence angle in mid-latitudes. In relation to the Košice city, Slovakia, this report summarises results of spatial and statistical analyses of the relationship between vegetation metrics derived from the satellite imagery of Sentinel 2 mission and the reference vegetation metrics derived from high-resolution 3-D digital representations of urban greenery. The results confirmed that Sentinel 2 multispectral imagery is strongly applicable for mapping annual phenological changes of vegetetation in urban landscape. Normalized difference vegetation index (NDVI) was the most suitable metrics to parameterize the urban greenery among the tested ones. Linear models (least squares regression) were applied to test for the relationship. Importantly, the NDVI derived from the Sentinel 2 imagery markedly correlated with canopy density derived from airborne and terrestrial laser scanning data. This correlation was positive, high and stable (Pearson's r about 0.8) after development of leaves. It was weak (below 0.4) before onset of the spring bud burst and after autumn senescence. The observation provided promising outcomes for the Sentinel 2 imagery to be used as a proxy for parameterizing vegetation transmittance in solar irradiation modelling and heat flux estimation in urban space.

The work described in this report was done under ESA Contract. Responsibility for the contents resides in the author or organisation that prepared it.

Names of authors: Michal Gallay, Jaroslav Hofierka

** NAME OF ESA STUDY MANAGER: DIV: DIRECTORATE:	** ESA BUDGET HEADING:

1 Introduction

1.1 Contractual

This document has been issued by Institute of Geography, P.J. Šafárik University in Košice for European Space Agency under contract Nr. 4000117034/16/NL/NDe titled "Simulating the cooling effect of urban greenery based on solar radiation modelling and a new generation of ESA sensors (acronym SURGE)".

1.2 Purpose of the Document

This document presents the results of spatial and statistical analyses of the relationship between vegetation metrics derived from the satellite imagery of Sentinel 2 mission and the reference vegetation metrics derived from high-resolution 3-D digital representations of urban greenery. The adopted methods relate to the D1 "Report on the reviewed applicability of multispectral satellite imagery for derivation of vegetation transmittance" and the D3 "Mid-term report" in which the data collection methods and generation of 3-D city model were described together with the time series of 3-D high resolution vegetation models in urban environment of the Košice City, Slovakia (Fig. 1). The here presented results address the following technical objectives (TO) as outlined in the proposal of the contract 4000117034/16/NL/NDe:

TO3: Derivation of reference vegetation metrics based on the time series of 3-D models of urban greenery and defining their correlation with vegetation metrics based on multispectral satellite imagery;

TO4: Downscaling the satellite vegetation metrics to high-resolution data based on the 3-D city model and 3-D greenery time series.

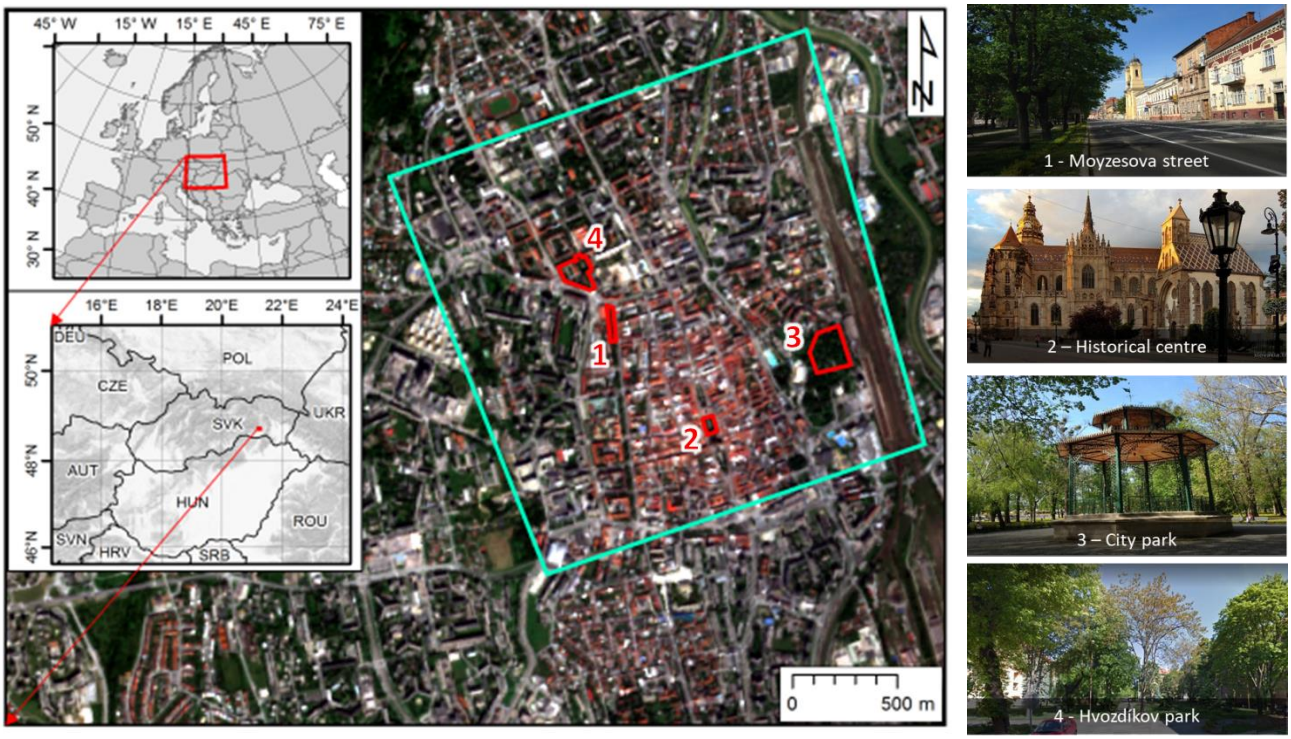

Figure 1. Location of the study area in the Košice City, Slovakia. The cyan line outlines the area subject to airborne lidar and photogrammetric mapping in a single mission, time series of the Sentinel 2 image coverage. The red outline delineates four sites selected for repeated terrestrial laser scanning of urban vegetation. The background maps are © Copernicus, Sentinel 2A image acquired on 7 September 2016.

1.3 Motivation

Radiation received at the urban surface is highly variable in space and time resulting from the complex form and land cover of urban environments. Understanding this variation in intercepted solar radiation is fundamental to determining various components of the urban energy landscape. Given the associations between vegetated land cover and the biophysical and social processes of urban systems there exists an ongoing demand for effective urban vegetation mapping and classification techniques (Tooke et al., 2009). The D1 report (SURGE_D1_SOA_MSVT) summarized supporting material from published studies why and how much vegetation in cities reduces solar radiation received by built-up areas. The most pronounced solar radiation loss determining the cooling of the local climate occurs during the summer time which is related to the full development of plants, especially trees with leaves. The D1 report also showed that the normalized vegetation index (NDVI) is most frequently used for efficient parametrization of vegetation conditions despite the known shortcoming with saturation of high NDVI values. In modelling the solar irradiation of urban space, both atmospheric transmittance and geometric structure of urban space were shown to be critical model parameters. For the purposes of assessing the vegetation transmittance, NDVI and other indices cannot be directly used. Metrics expressing the nature of vegetation transmittance for the solar radiation comprise, for example, leaf area index (LAI), canopy cover, tree canopy closure, canopy gap fraction, etc. However, these are difficult to be measured directly from the satellite imagery. It has been shown by many studies that, into certain extent, NDVI and other indices are correlated with the metrics and can be used as a proxy for their calculation. Tooke et al. (2012) propose that opportunities exist for incorporating additional spectral data, especially for generating estimates of the reflected component of incoming solar radiation. The potential also exists for advancing estimates of radiation transmission by articulating the temporal, spectral and structural dynamics of the local vegetation. The multispectral imagery acquired by the Sentinel 2 mission has relatively high spatial, spectral and temporal resolution to capture the dynamic of vegetation phenology. But are the properties of this data sufficient to be used as a proxy of the vegetation transmittance on higher resolution? This report addresses this question.

1.4 Land surface temperature and vegetation

The availability of multispectral imagery including a thermal infrared band enabled monitoring the spatial pattern of land surface temperature (LST) and linking it with land cover properties. Multispectral data archives allow for assessing the dynamics of urban heat island (UHI) by the means of LST mapping for particular area. The research on UHI has been focused on large cities where the phenomenon is the most pronounced. However, UHI concerns also smaller cities which are more abundant and over a half of urban population lives in cities with less than a half of million inhabitants. The city of Košice is an example of a typical small post-communist Central European city after changes of urban landscape induced by transition to capitalism and modern trends in economy. We demonstrated the urban greenery has on the distribution of LST and the existence of the UHI phenomenon in Košice. We determined differences in the LST distribution in the city under various weather conditions in the vegetation season from 2013 to 2015. The data used comprised ground-based weather station data and the Landsat 7 and Landsat 8 imagery for deriving LST and NDVI. Figure 2 compares the spectral resolution and spectral range of the bands for the satellites and Sentinel 2 which does not provide thermal sensing. The results are summarised in Onačillová & Gallay (2018) and revealed the spatial pattern of the LST and UHI in Košice supporting the hypothesis that UHI poses a problem even in such a small city. Expansion of urban fabric by construction of new residential, commercial and industrial estates and also building new traffic infrastructure in last few years amplified the UHI. Strong correlation was calculated

between the LST and the amount of urban greenery in the city expressed by NDVI (Fig. 3). The graphs indicate that the linear relationship is strong during the vegetation season. Even narrow green alleys or small parks are capable of mitigating the UHI phenomenon which can be well seen in Fig. 4. Also, the relation between cooler LST spots in the city centre and patches of green vegetation (high NDVI values) can be visually clearly identified. The findings of this study can serve as useful arguments for officials in Košice but also in other cities to support investments in development of green areas.

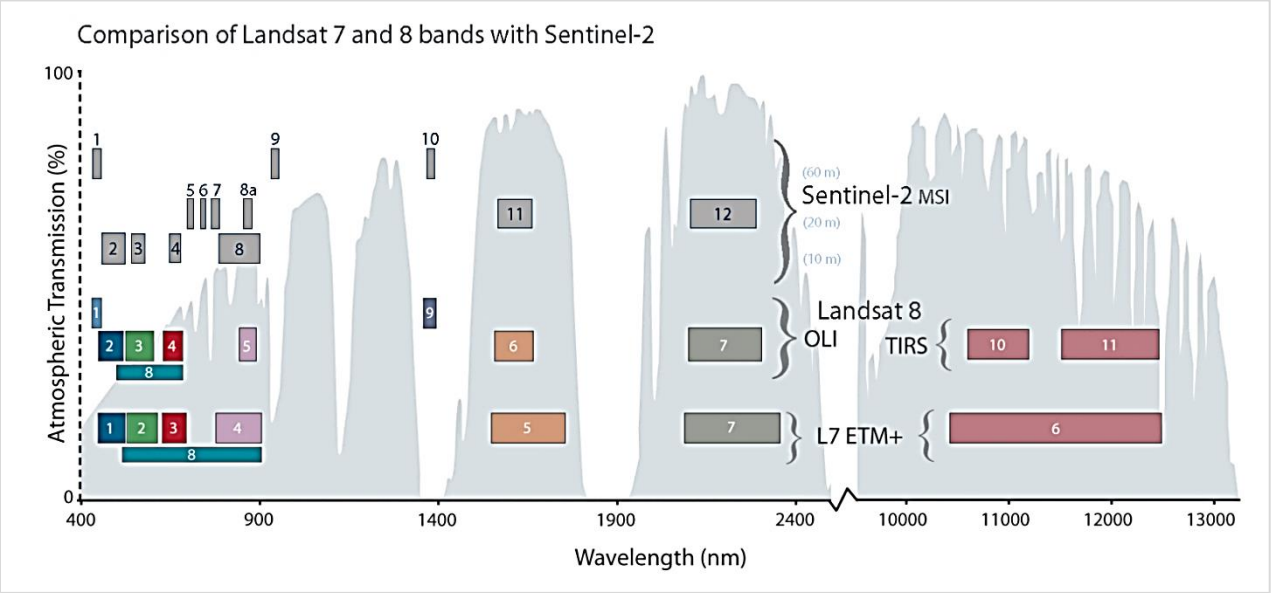

Figure 2. Comparison of spectral and spatial resolution of the Landsat 7 ETM+, Landsat 8 OLI/TIRS and Sentinel 2 MSI sensors. Source: http://landsat.gsfc.nasa.gov/sentinel-2a-launches-our-compliments-our-complements/

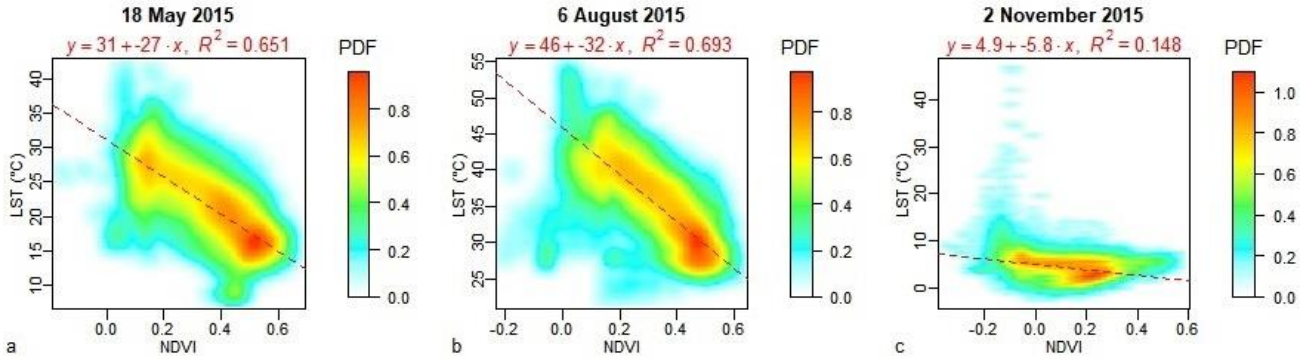

Figure 3. Smoothed scatterplots of LST and NDVI from Landsat 8 OLI/TIRS scenes in the administration area of Košice for three selected dates in spring, summer and late autumn. For high density of points in the scatterplots, the points are expressed as the values of probability density function (PDF) resulting from a two-dimensional kernel density estimation. Each scatterplot comprises a linear regression model. Adopted from Onačillová & Gallay (2018).

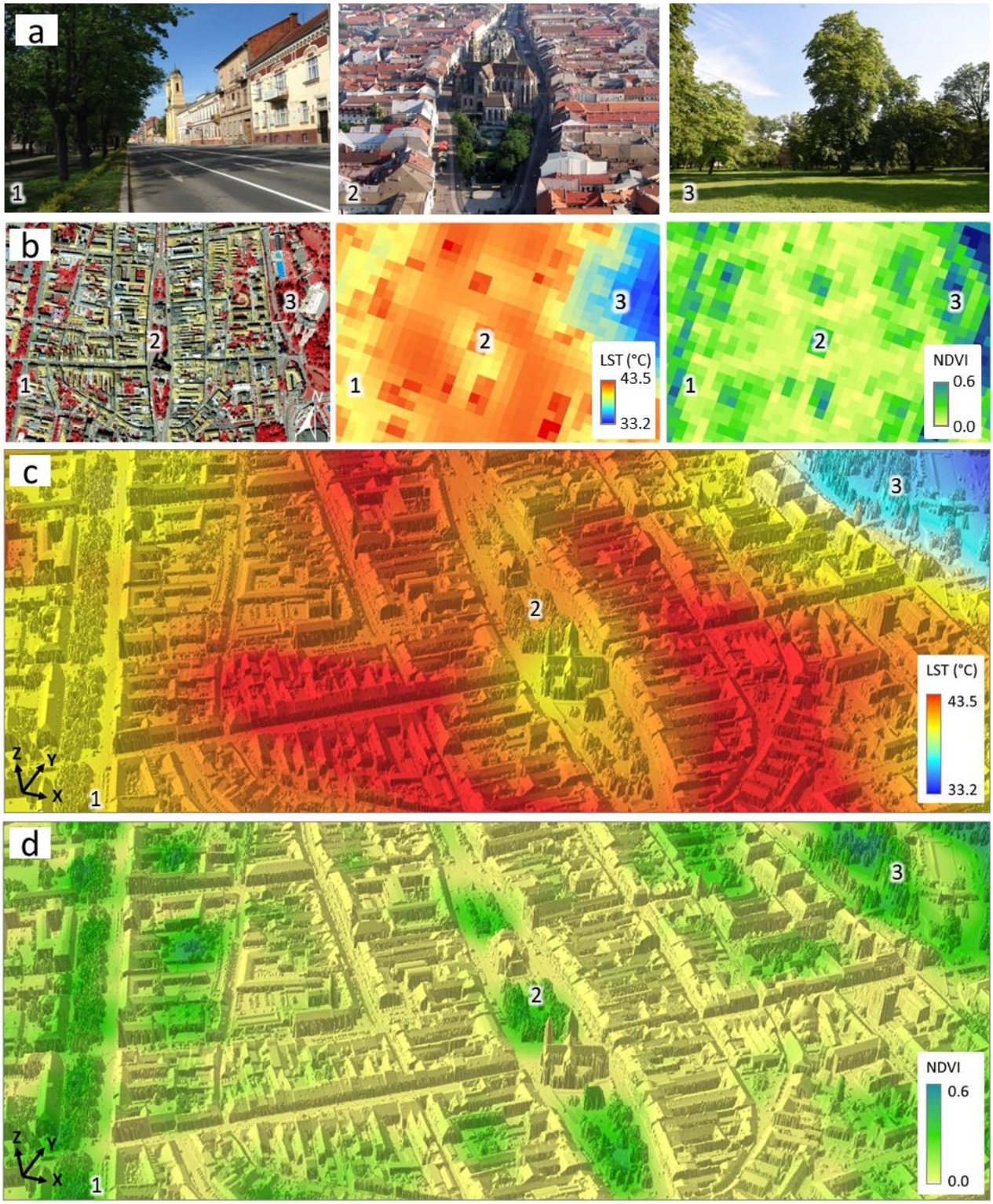

Figure 4. LST and NDVI values derived from Landsat 8 OLI/TIRS scene acquired on 6 August 2015 for selected areas of the historical city centre of Košice (A): 1 – green alley on Moyzesova Street, 2 – the core of the city-centre, 3 – city park. (B) perspective 3D view of the LST model resampled to 0.5 m resolution draped over the lidar based digital surface model described in Hofierka et al. (2017). Figure adopted from Onačillová & Gallay (2018).

2 Data

Selected vegetation metrics were derived from spaceborne multispectral imagery of Sentinel 2A and Landsat 8 satellites, by airborne photogrammetry, airborne laser scanning, and terrestrial laser scanning (Fig. 5). Sentinel 2 mission and data were specified in the D1 report and the other types of datasets in the D3 report. Therefore here, we specify only the details important for the presented analyses. While spaceborne multispectral imagery and airborne datasets were acquired for the entire study area (Fig. 1, cyan outline), the terrestrial lidar data were collected only within four smaller sites (Fig. 1, red outline).

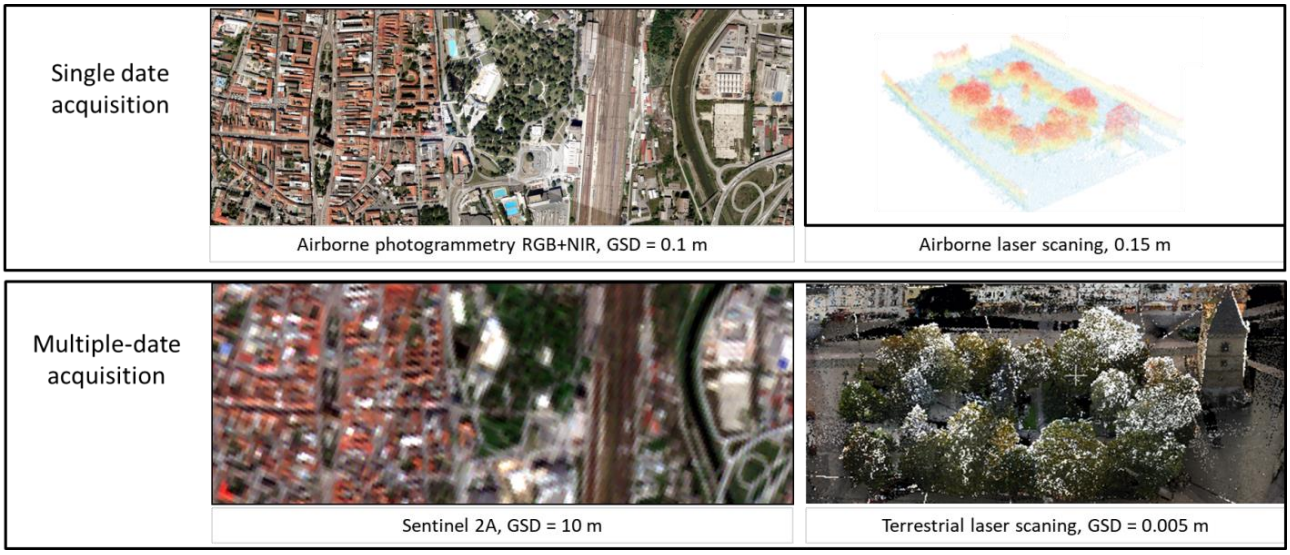

Figure 5. Samples of data used in the presented report for derivation of vegetation metrics and their spatial and temporal resolution.

2.1 Sentinel 2A MSI data

The Sentinel-2 mission is a land monitoring constellation of two satellites Sentinel 2A and Sentinel 2B that provide multispectral scenes comprising 13 spectral bands in the range of visible to middle infra-red spectrum (Fig. 2). In this report, we have used the Sentinel 2A bands 2, 4, and 8 having 10 m spatial resolution (Tab. 1). The study area is covered by two Sentinel 2A data granules 34 UEU, 34 UEV which were downloaded for the year of 2016 via Copernicus Open Access Hub (https://scihub.copernicus.eu/dhus/). The time period corresponded with the acquisition of the other datasets. The data were distributed as level 1C products meaning the pixel values represent the top-of-atmosphere spectral reflectances projected in a cartographic system (UTM/WGS84).

Table 1. Spectral bands of the Sentinel 2A Multispectral Instrument (MSI) used in this study

Band number	Wavelength [μm]	Central Wavelength (μm)	Resolution (m)
2	0.440 - 0.538	0.490	10
4	0.646 - 0.684	0.665	10
8	0.760 - 0.908	0.842	10

2.2 Landsat 8 OLI/TIRS data

The imagery of the Landsat 8 mission, managed by the U.S. NASA and USGS, was used to compare the vegetation metrics with those derived from Sentinel 2A data. Relation of thermal properties of the land surface and NDVI were discussed in Section 1.4 and by Onačillová & Gallay (2018) and they were not subject of the analyses in this report. The study area is situated within two Landsat 8 data scenes (path 186, row 26, and path 187, row 26). Data were downloaded from the USGS web geoportal (https://earthexplorer.usgs.gov/) for dates as close as possible to the dates of Sentinel 2A acquisition. The bands involved in calculation of vegetation metrics and land surface temperature are specified in Table 2. The data were acquired as level 1 product in which the pixel values represented scaled digital numbers (DN) of spectral radiance at the top-of-atmosphere projected in a cartographic system (UTM/WGS84).

Table 2. Spectral bands of Landsat Operational Imager (OLI) and Thermal Infrared Sensor (TIRS) used in this study

Band number	Wavelength [μm]	Resolution [m]
4 (OLI)	0.64 – 0.67	30
5 (OLI)	0.85 – 0.88	30
10 (TIRS)	10.60 – 11.19	100

2.3 Airborne photogrammetry data

Photogrammetric imagery was collected in 4 spectral bands (blue, green, red, near infra-red) in a single mission flown on 9 August 2016 under leaf-on conditions by Vexcel UltracamXp digital camera resulting two natural and NIR false colour orthoimagery with spatial resolution of 10 cm. For mapping the urban greenery in the entire study area airborne laser scanning data coupled with NIR false colour photogrammetric imagery was used. The airborne laser scanning (ALS) points representing the vegetation were extracted by classification based on point heights and by thresholding the RGB values from the NIR colour composite. The orthoimagery was supplied in the national cartographic projection system S-JTSK Krovak East North (EPSG: 5514) and also in UTM/WGS84.

2.4 Airborne laser scanning data

This data were acquired in a single mission on 14 September 2016 under leaf-on conditions with a Leica ALS70-CM lidar system with other specifications listed in Table 3. The raw point data were supplied in the national cartographic projection system S-JTSK Krovak East North (EPSG: 5514) and also in UTM/WGS84. The points were processed in LAStools to classify them in ground, vegetation, buildings and other returns. Ground returns were used to derive a gridded digital terrain model (DTM) and digital surface model (DSM) of 0.2 m cell size. The orthoimagery was supplied in the national cartographic projection system S-JTSK Krovak East North (EPSG: 5514) and also in UTM/WGS84.

Table 3. Parameters of the ALS mission flown with a Leica ALS70-CM lidar system.

Parameter	Value
Flight height above ground	1050 - 1087 m
Flight altitude above mean sea level	1,333 m
Total number of points	365 million

Total area	4 km^2
Average density of returns (all/ground)	91 / 15 points per m^2
Absolute overall accuracy in open areas	0.1 m @ 1σ

2.5 Terrestrial laser scanning data

We have selected four smaller test sites covering several hectares (Fig. 1, red outlines) for detailed mapping of urban vegetation and its geometric change using repeated terrestrial laser scanning (TLS). Each site represents typical urban greenery consisting of various kinds of trees of different height. The TLS of urban greenery was done in the four study sites during the period April – November 2016 and in March 2017 using a RIEGL VZ-1000 scanner equipped with a Nikon D700 camera. The aim of the scanning was to capture vegetation in several phenological phases synchronously with the Sentinel 2A overflight times (+/- 1-2 days) taking into account meteorological conditions.

TLS resulted in 44 datasets (point clouds) with total size of 93.8 GB representing the study sites in 11 time horizons during one vegetation period. TLS required selection of appropriate positions of the scanner during the survey in order to minimize data shadows and total number of required positions. At the same time, it was important to ensure a sufficient overlap with the adjacent position. Final mutual registration of individual point clouds was performed using the Multi-Station Adjustment implemented in the RiSCAN Pro software by the means of planar patches identified on buildings and other stable objects which have not moved during the period of scanning, thus not on vegetation. Mean standard deviation of adjusting the scans for a particular site and date of scanning was in the order of centimetres. The point cloud was also colourized using the digital RGB imagery acquired immediately after scanning with the integrated camera (Fig. 5). The TLS data was georeferenced in the national cartographic projection system S-JTSK Krovak East North (EPSG: 5514) by the means of ground control points located by a dual frequency RTK-GNSS receiver during the first scanning data on each site with accuracy in the order of 1-2 centimetres. Overview and images of the TLS time series can be seen on the project website http://esa-surge.science.upjs.sk/index.php/study-sites. A summary was provided in Progress Report 1, Table 1 and in the D2 report.

3 Methods

3.1 Data pre-processing

The objective of this report was to link the spectral response of urban vegetation in Košice with geometric structure of the vegetation. The spatial datasets described in Sections 2.1-2.4 were clipped by the polygon of the study area (Fig. 1, cyan outline) and also by the polygons of the four smaller sites (Fig. 1, red outline). To make the TLS point data acquired on different dates comparable in terms of the recorded number of points, the point clouds from each date of acquisition were decimated by an octree-based filter so that only a single lidar return point remains in a 1 cm^3 voxel. This resolution was empirically tested and provided optimal differentiation of the seasonal change of vegetation. ALS and TLS data were cleaned so that points remained only within the tree canopy footprints (Fig. 6).

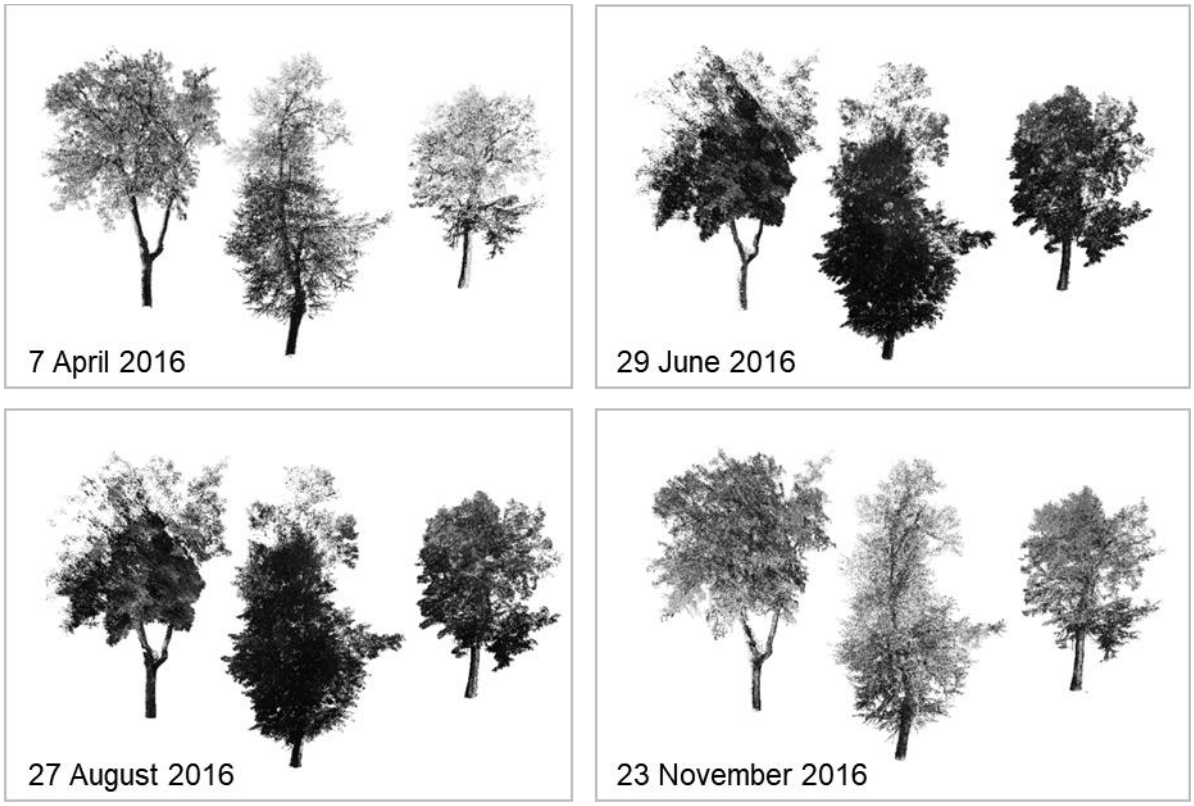

Figure 6. Example of TLS point clouds of trees from the site of Moyzesova street in 4 time aspects.

3.2 Vegetation metrics from multispectral data

Green vegetation has a very specific spectral response enabling to distinguish photosynthetically active (green) vegetation from other land cover types. The D1 report summarized some of the important vegetation indices used for mapping vegetation transmittance or area covered by vegetation. Once the area covered by vegetation is outlined metrics assessing the spatial pattern of vegetation cover can be used. Based on the generated review in the D1 report, we have selected four widely used indices making use of raster map algebra, band combinations, or thresholding of values recorded in particular band. The formulas of the indices are listed in Table 4 with the Sentinel 2A bands which were used for calculation of the indices. The formulas were defined in the https://www.indexdatabase.de by Henrich et al. (2012). Before calculation of the indices, the original Sentinel 2A data were divided by the scaling factor of 10,000 which is used to store the reflectance data as integers. There was only NDVI derived from orthoimagery.

Undoubtedly, the normalized vegetation index (NDVI), and its refined form, enhanced vegetation index (EVI), is the most widely used for continental to global - scale vegetation monitoring because it can compensate for changing illumination conditions, surface slope, and viewing angle (Jensen, 2006). The principle of applying NDVI in vegetation mapping is that vegetation is highly reflective in the near infrared and highly absorptive in the visible red. The contrast between these channels can be used as an indicator of the status of the vegetation. There is also another type of enhanced vegetation index (EVI2) which avoids the use of blue band (Jiang et al., 2008). Soil Adjusted Vegetation Index (SAVI) was another calculated index originally defined by Huette et al. (1988).

Table 4. Formal definition of vegetation indices

Vegetation index	Formulas
NDVI	(NIR-R) / (NIR+R)
EVI	2.5 * (NIR - R) / (NIR + 6 * R - 7.5 * B + 1)
EVI2	(2.5 * (NIR – R)) / (NIR + (2.4 * R) + 1)
SAVI	(1.5 * (NIR - R) / (NIR + R + 0.5))

Sentinel 2: B = Band 2, R = Band 4, NIR = Band 8; Landsat 8: B = Band 2, R = Band 4, NIR = Band 5; orthoimagery: B = blue band, R = red band, NIR = near infra-red band.

3.3 Vegetation metrics from laser scanning data

For the purposes of assessing the vegetation transmittance, NDVI and other indices cannot be directly used. Metrics expressing the nature of vegetation transmittance for the solar radiation comprise, for example, leaf area index (LAI), canopy cover, tree canopy closure, canopy gap fraction, etc. However, these are difficult to be measured directly from the satellite imagery. It has been shown by many studies that, into certain extent, NDVI and other indices are correlated with the listed metrics and can be used as a proxy for their calculation. Airborne (ALS) and terrestrial (TLS) laser scanning data were used to derive vegetation canopy density (CD), canopy cover (CC) and effective leaf area index (LAI_e).

The canopy density was calculated as follows:

$$CD = R_v/A$$

Where R_v is the number of vegetation lidar returns situated 1.37 m above the ground per cell area. We used 0.1 m and 10 m cell area.

The canopy cover (CC) was calculated as follows:

$$CC = R_a / R_b$$

where R_a is the number of lidar points situated 1.37 m above the ground, R_b is the number of points below this threshold height.

Recent studies have indicated the possibility to use aerial LiDAR to map LAI_e in a heterogeneous urban park (Richardson et al., 2009) and in an urban environment (Alonzo et al., 2015). To estimate LAI_e from ALS and TLS data, the following approach by Klingberg (2017) based on Beer-Lambert law was used:

$$LAI_e = - \beta \, . \, ln(R_{ground} / R_{total})$$

where R_{ground} is the number of ground returns (including all return types), R_{total} is the number of ground and canopy returns and β is a constant. β can be expected to take a value around 2, which is the theoretical value given that the foliage angle distribution is spherical and that the penetration

rate of laser pulses is equal to vertical gap fraction. Richardson et al. (2009) tested four different methods to estimate LAI_e from lidar data in a mixed forest in Seattle, USA and found the above described method to give the best result. The values of LAI_e tend to range from 0 for bare ground to 6 for ground covered by dense vegetation. We calculated the LAI_e and CC for grid cells of 10 by 10 metres to match the resolution of Sentinel 2A imagery.

4 Results

4.1 Basic statistics of urban greenery

Based on the airborne photogrammetric and laser scanning data the calculated green vegetation covers about 23% of the study area. The mean height of vegetation above 0.1m is 8.4 m with standard deviation of 6 m. The highest trees reach up to 36 m but half of them is lower than 10 m. Figure 7 depicts the spatial distribution of the vegetation height above ground. The vegetation in the four small sites that were subject to TLS survey comprises 83% of deciduous species and 17% of coniferous species. Details are provided in Table 5.

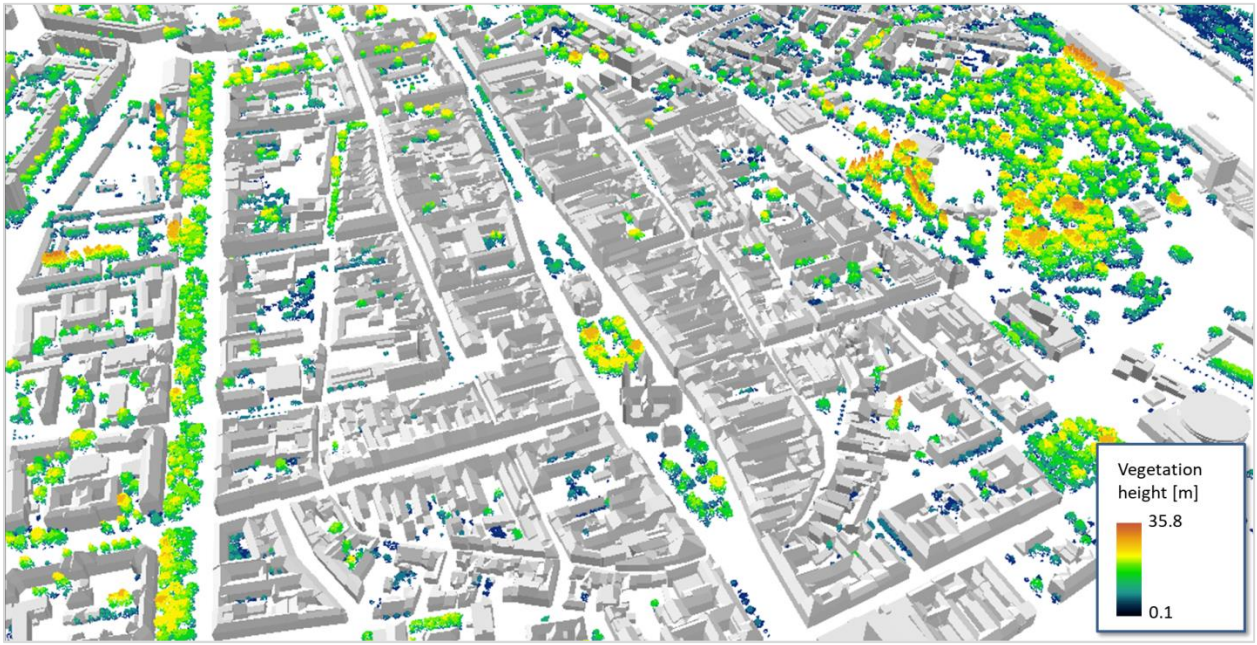

Figure 7. Perspective view of the 3-D city model of the study area with trees and shrub vegetation coloured by height above ground.

Table 5. Tree and shrub vegetation species within the four small sites (Fig. 1, red outline)

Tree and shrub species	**Count**	**Percentage**
Tilia cordata	102	17,6
Acer platanoides	87	15,0
Betula pendula	61	10,5
Aesculus hippocastanum	37	6,4
Acer pseudoplatanus	25	4,3
Picea abies	25	4,3
Gleditsia triacanthos	24	4,1
Acer negundo	22	3,8
Picea pungeus	21	3,6
Pinus nigra	16	2,8
Robinia pseudoacacia	12	2,1
Thuja orientalis	12	2,1
Catalpa bignonoides	11	1,9
Acer saccharum	9	1,5
Tilia platyphyllos	9	1,5
Abies alba	8	1,4
Carpinus betulus	7	1,2
Ailanthus altissima	6	1,0
Fraxinus excelsior	5	0,9
Platanus occidentalis	5	0,9
Syringa vulgaris	5	0,9
Taxus bacatta	5	0,9
Celtis occidentalis	4	0,7
Liriodendron tulipifera	4	0,7
Magnolia liliflora	4	0,7
Platanus orientalis	4	0,7
Quercus rubra	4	0,7
Thuja occidentalis	4	0,7
Cerasus avium	3	0,5
Fraxinus ornus	3	0,5
Chamaecyparis pisifera	3	0,5
Prunus cerasifera	3	0,5
Ulmus laevis	3	0,5
Corylus avellana	2	0,3
Cupressus sempervirens	2	0,3
Fagus sylvatica	2	0,3
Lonicera xylosteum	2	0,3
Negundo aceroides	2	0,3
Quercus robur	2	0,3
Salix alba	2	0,3
Sophora japonica	2	0,3
Other species as a single occurrence - Abies procesa, Juglans regia, Juniperus communis, Larix decidua, Morus nigra, Morus rubra, Picea glauca , Pinus strobus, Platanus hispanica, Potentilla fruticose, Salix babylonica, Sambucus nigra	12	2.4
Total	581	100,0

4.2 Relation between vegetation metrics derived from multispectral imagery

The derived NDVI, EVI, EV2, SAVI indices were visually compared for various dates which indicated no marked difference in the pattern of vegetation distribution (Fig. 8). Scatterplots of the indices and fitted linear regression model indicated strong correlation between the indices (Fig. 9). NDVI is not based on any constant parameters which have to be empirically estimated for the inspected area. The EVI, EVI2 and SAVI involve such parameters. For these reasons, we decided to further define the relationship between the NDVI and vegetation metrics derived from lidar data.

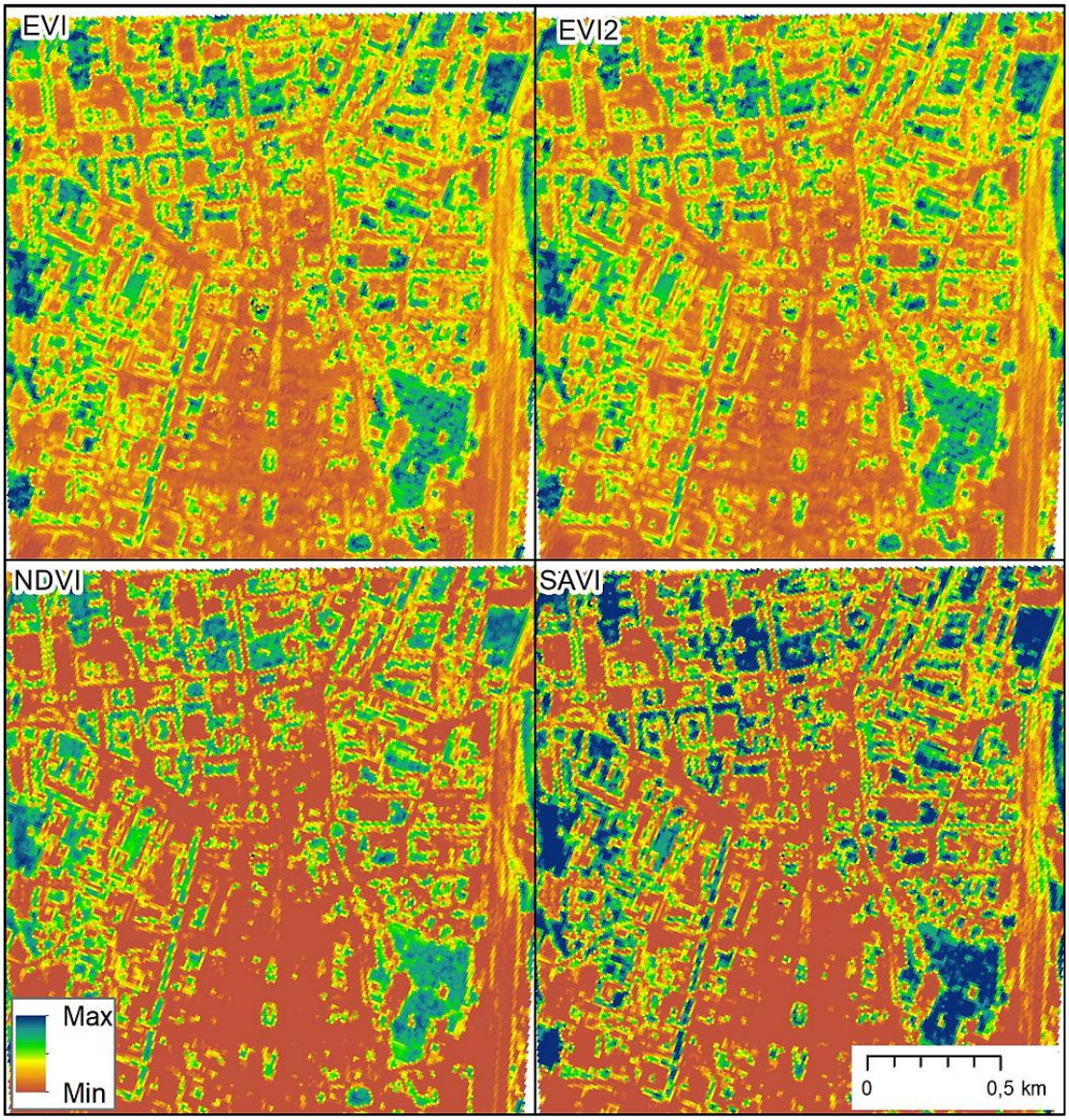

Figure 8. Four vegetation indices derived from Sentinel 2A data acquired on 8 August 2016.

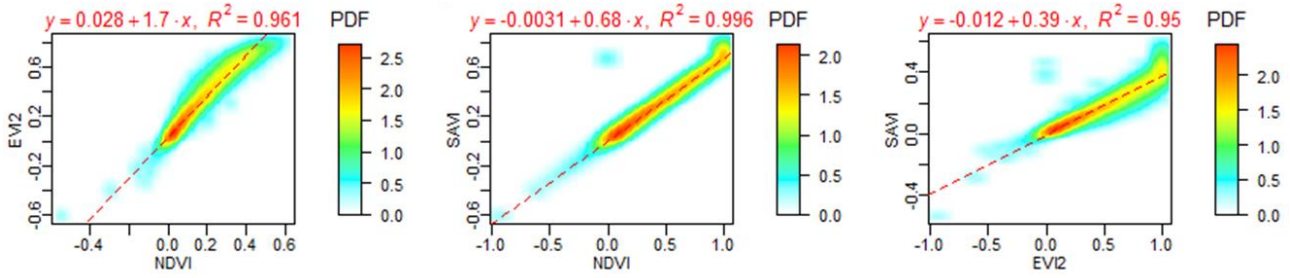

Figure 9. Smoothed scatterplots and linear regression model for combinations of vegetation indices NDVI, EVI2, SAVI derived for the extent of the study area (Fig. 1, cyan outline) at 10 m spatial resolution from imagery of Sentinel 2A. Date of sensing: Sentinel 2: 8 August 2016.

NDVI is a biophysical parameter that correlates with photosynthetic activity of vegetation. In addition to providing an indication of the 'greenness' of the vegetation, NDVI is also able to offer valuable information of the dynamic changes of specific vegetation species given that multiple-time images are analyzed. Therefore, NDVI is a good indicator to reflect periodically dynamic changes of vegetation groups. However, NDVI should be interpreted with care as its values exhibit nonlinear relationships with biophysical measures, such as LAI or vegetation fraction. While NDVI reaches a maximum it does not increase despite continued increases in LAI or biomass (Campbell and Wynne, 2011).

4.3 NDVI from Sentinel 2 and TLS canopy density

Canopy density takes into account the number of lidar returns over a horizontal areal unit. Figure 10 shows the density of TLS returns over the footprints of tree canopy per 10 by 10 cm grid cells on one site. Clearly, the rapid change during the transition of dormant season and the vegetation period is followed by stable density of points, i.e. penetration of laser light from the ground up in the direction of the laser beam. This levelled scenario changes after the fall of leaves in autumn. But, the change of the canopy density is not as marked with respect to spring. This simple analysis of time series of unified TLS point cloud suggests that the vegetation transmittance between the leaf-on and leaf-off stages changes by a factor of about 2.5.

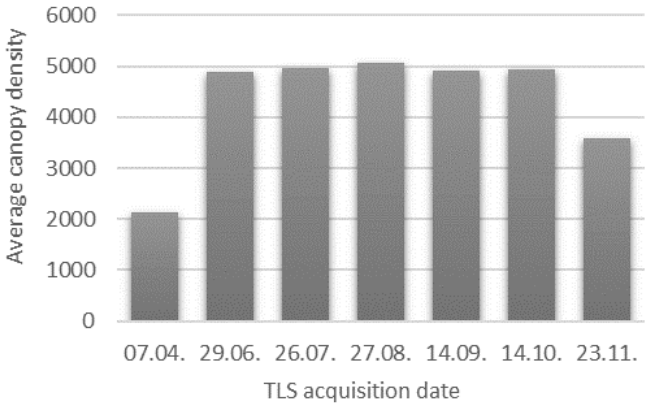

Figure 10. Temporal change of canopy density per 10 m grid cell for the site of Moyzesova street.

Figure 11 visually demonstrates the change of canopy density at the Moyzesova street site and its relation with the NDVI derived from Sentinel 2A imagery. The raster maps suggest that the two parameters are correlated, but the linear models shown in Figure 12 portray only medium linear correlation in June and weak in other months as inferred from relatively low values of R^2. Nevertheless, the graphs demonstrate that the strength of the linear relationship changes with the season and it seems to be strongest at the end of spring when the vegetation should be in the best condition.

The comparison of relation between NDVI and ALS and TLS derived canopy density for the same date (14 September 2016) showed that the canopy density seems to have similar strength of the relationship as calculated from the ALS data and TLS data (Fig. 13). This indicates that ALS data acquired in a single mission could be used to approximate the canopy density in a similar way than with TLS data. The change of canopy density could be inferred from ALS data using the prediction of linear models derived from TLS data. However, the potential of the linear models to explain the variation in the point based canopy density by NDVI derived from Sentinel 2 imagery is only about 30-40% (R^2). Anyway, the linear relationship is not convincing as a dense group of points in the graph concentrates in two opposite parts. Nevertheless, in each month high NDVI values are related with high canopy density.

Figure 11. Canopy density per 0.1 m cell from TLS data and Sentinel 2A NDVI for 10 m cell size for the site of Moyzesova street.

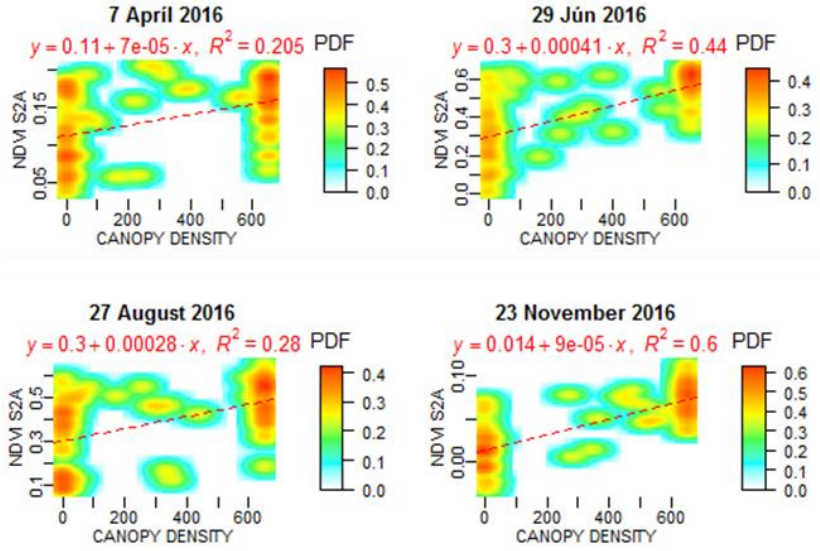

Figure 12. Smoothed scatterplots of Sentinel 2A NDVI and TLS canopy density calculated at 0.1 m grid cell size for the site of Moyzesova street.

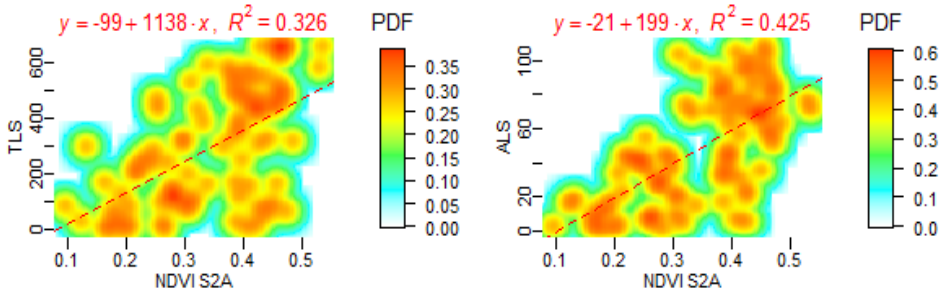

Figure 13. Smoothed scatterplots of Sentinel 2A NDVI and TLS canopy density calculated at 10 m grid cell size for the site of Moyzesova street. Data acquired on 14 September 2016.

4.4 NDVI from Sentinel 2 and TLS canopy cover

Canopy cover defines ratio of how many points are above 1.37 metres to the number of points below this height, which is meant to be the bottom height of a tree crown. The linear models and smoothed pattern of the XY points within the graph indicate that the canopy cover parameter does not provide convincing relation with the NDVI of Sentinel 2A. Despite the correlation is very weak, the tendency of high NDVI values related with high values of canopy cover is clearly visible.

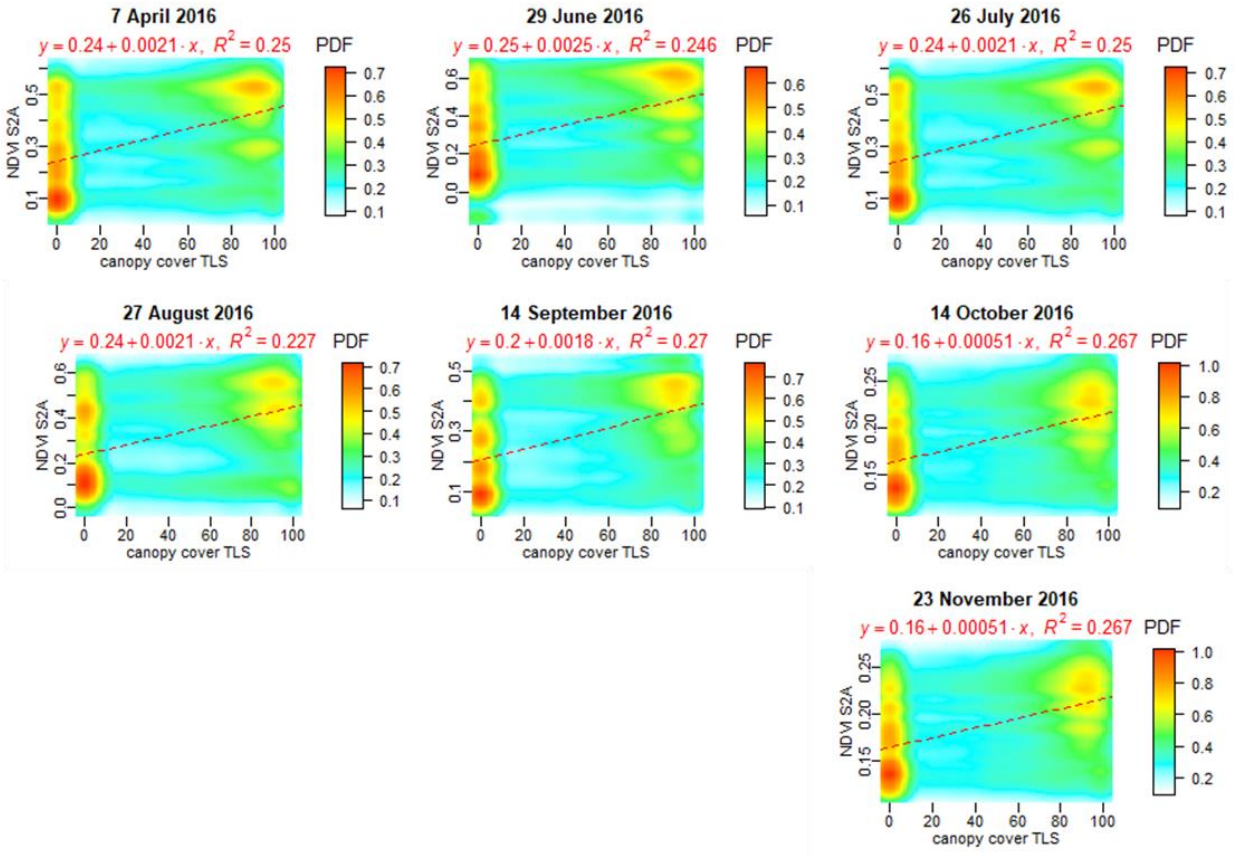

Figure 14. Smoothed scatterplots of NDVI and TLS canopy cover calculated at 0.1 m grid cell size for the site of Moyzesova street.

4.5 NDVI from Sentinel 2 and TLS LAI_e

The estimated leaf area index appears to be a more suitable vegetation metric from the three calculated parameters to relate the change of NDVI with geometric structure of the tree vegetation. Figure 15 shows the spatial distribution of LAI_e and NDVI in four selected months in Moyzesova street. The change of LAI_e is not visually apparent in contrast to NDVI. However, Figure 16 shows that the correlation is strong the linear correlation of TLS based LAI_e and Sentinel 2 based NDVI is very weak in leaf-off conditions (spring) and strong in the leaf-on conditions, when the variation in LAIe explains over 50% of the variation in NDVI. The highest values of LAIe tend to be co-located with the highest values of NDVI and vice versa; similarly, as with the canopy density and canopy cover. Figure 17 shows the pattern of both parameters for other two sites in August visually indicating the influence of other kind of surfaces in the NDVI value. The site of Hvozdíkov park comprises 20 m tall trees which do not maintain continuous tree cover with each other. Figure 18 demonstrates this finding in the scatterplots, the density of XY points is more dispersed around the linear trend in Hvozdikov park than in other three sites. Despite the ALS based data are used as the response variable, it indicates the problem of mixing reflectance of vegetation canopy with reflectance of other surfaces within a single pixel.

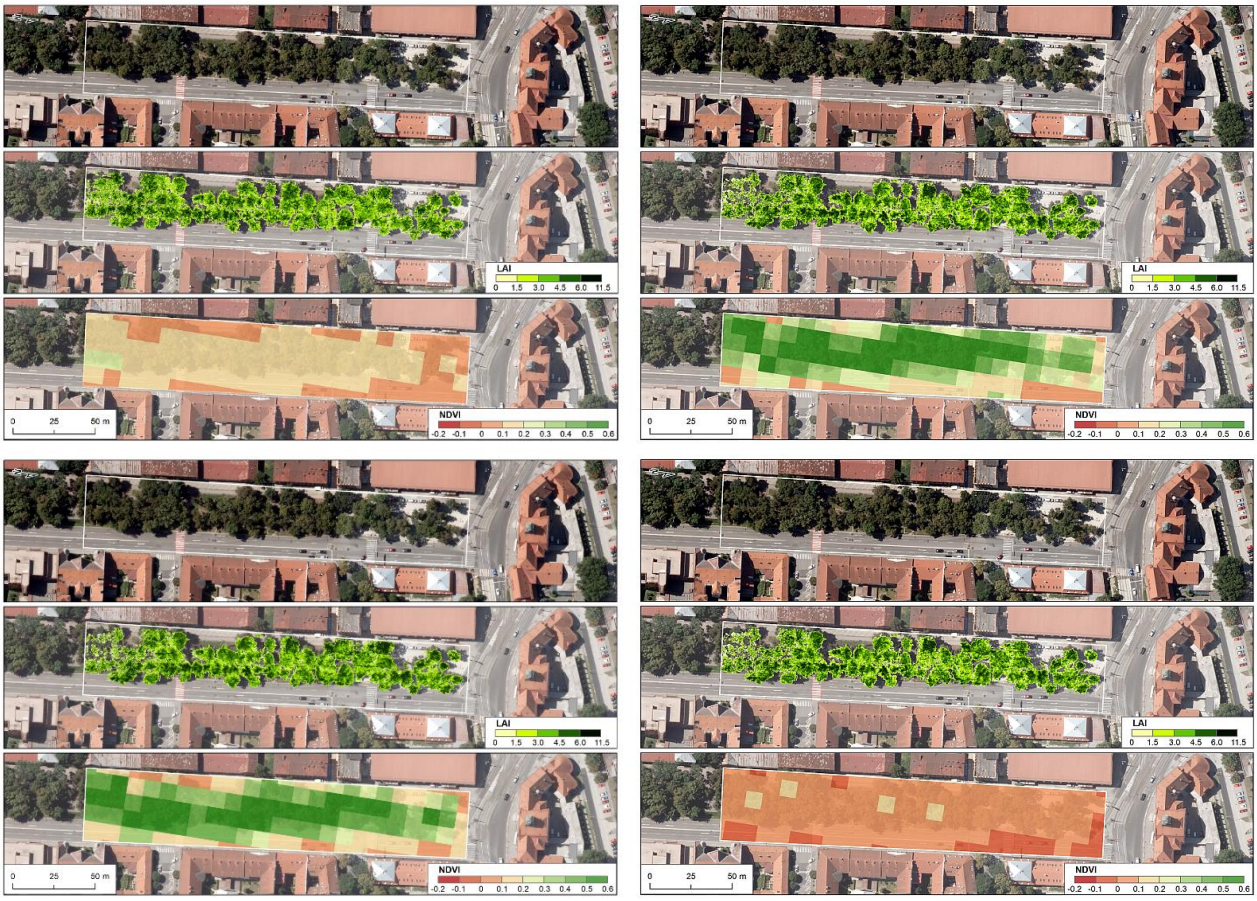

Figure 15. LAI_e per 0.1 m cell size from TLS data and Sentinel 2A NDVI for 10 m cell size for the site of Moyzesova street. Data acquisition: 7 April 2016 (top left), 26 July 2016 (top right), 27 August 2016 (bottom right), 23 November 2016 (bottom right).

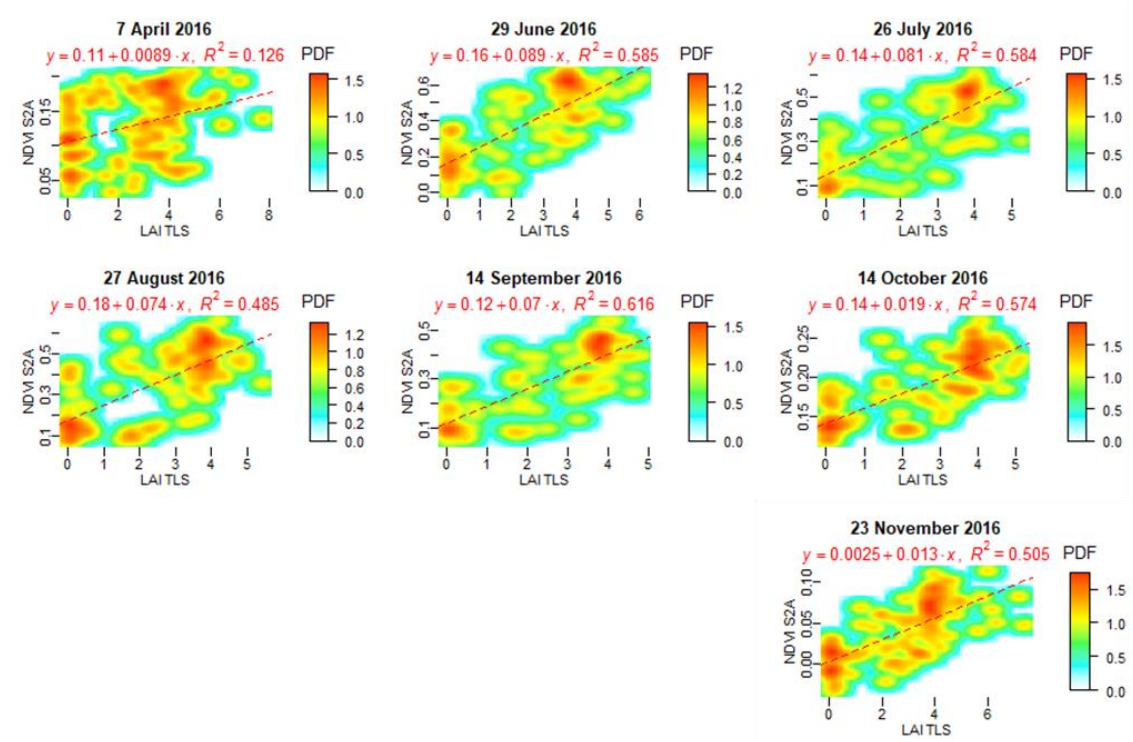

Figure 16. Smoothed scatterplots of Sentinel 2A NDVI and LAI_e canopy density calculated at 0.1 m grid cell size for the site of Moyzesova street.

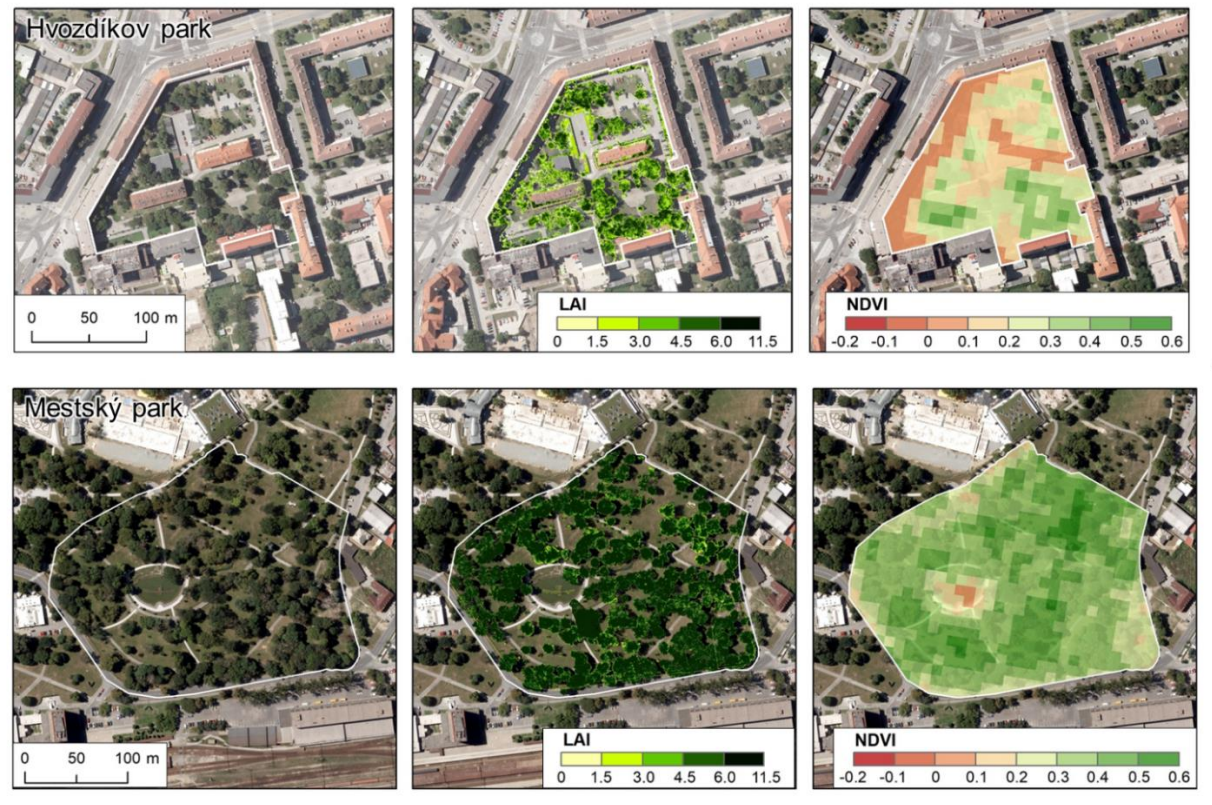

Figure 17. LAI_e per 0.1 m cell size from TLS data and Sentinel 2A NDVI for 10 m cell size for the site of Hvozdíkov park and Mestský park. Data acquisition: 27 August 2016.

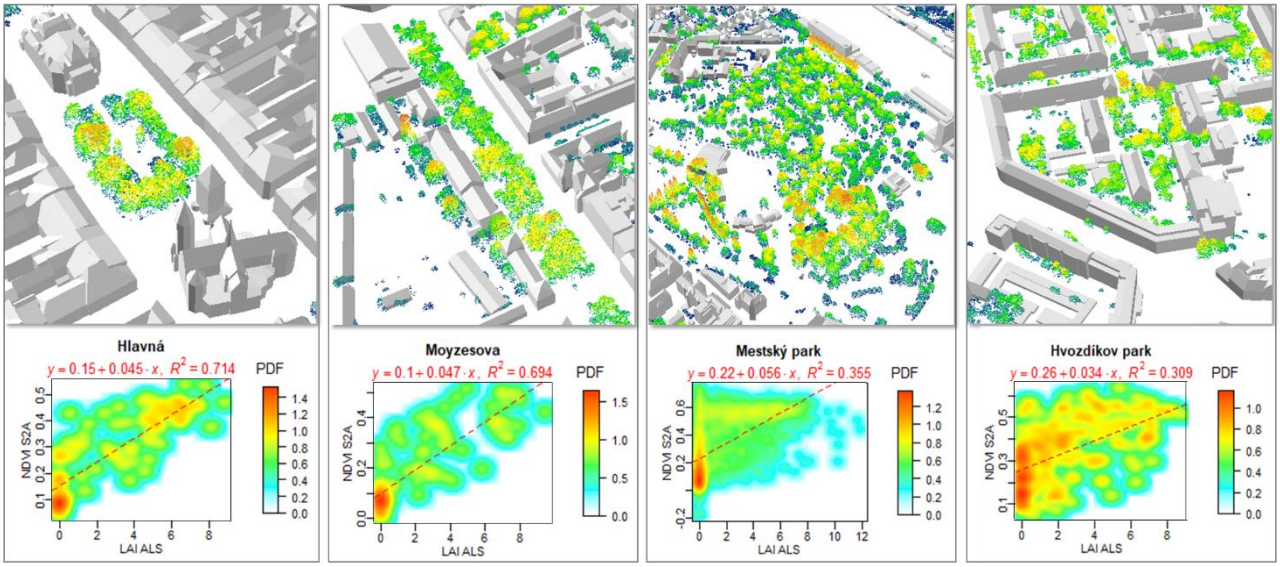

Figure 18. LAI_e per 10 m cell size from ALS data and Sentinel 2A NDVI for 10 m cell size for all four small sites. Data acquisition: 14 September 2016.

4.7 Relating ALS and TLS based LAI_e

The change of geometric structure of vegetation was measured by TLS and the derived time series of TLS point clouds were related to NDVI of Sentinel 2. The ultimate goal is to define vegetation transmittance by only having ALS point cloud and Sentinel 2 data as inputs for solar irradiation modelling with considering the vegetation transmittance in different seasons. Therefore, we need to bridge the linear models of TLS and Sentinel based metrics with the ALS data. For this task, we tested how the LAI_e from TLS relates with LAI_e based on ALS data which is displayed by Fig. 19. The graph shows that the explanatory power of ALS based LAI_e for explaining the TLS based LAI_e is strongest when the resolution used to derive the LAI_e is between 8 – 10 meters where R^2 is above 0.6 indicating strong linear correlation. Such spatial resolution corresponds with the spatial resolution of the Sentinel 2 bands, which were used in the presented research. Thus, it provides support that application of Sentinel 2 data for estimating seasonally varying vegetation transmittance could be possible and applicable for modelling the cooling effect of urban greenery with the proposed approach.

4.8 Spatio-temporal analysis of shadowing in high resolution

Implications of these results are manifested in the analysis of shaded area shown in Fig. 20. It is clear that for the selected site and time interval the effect of ground shadowing can be calculated using the generated time series of the meshed 3-D tree models. The time duration of area being shaded depends not only on the sun declination but also on the effect of the tree phenology is involved.

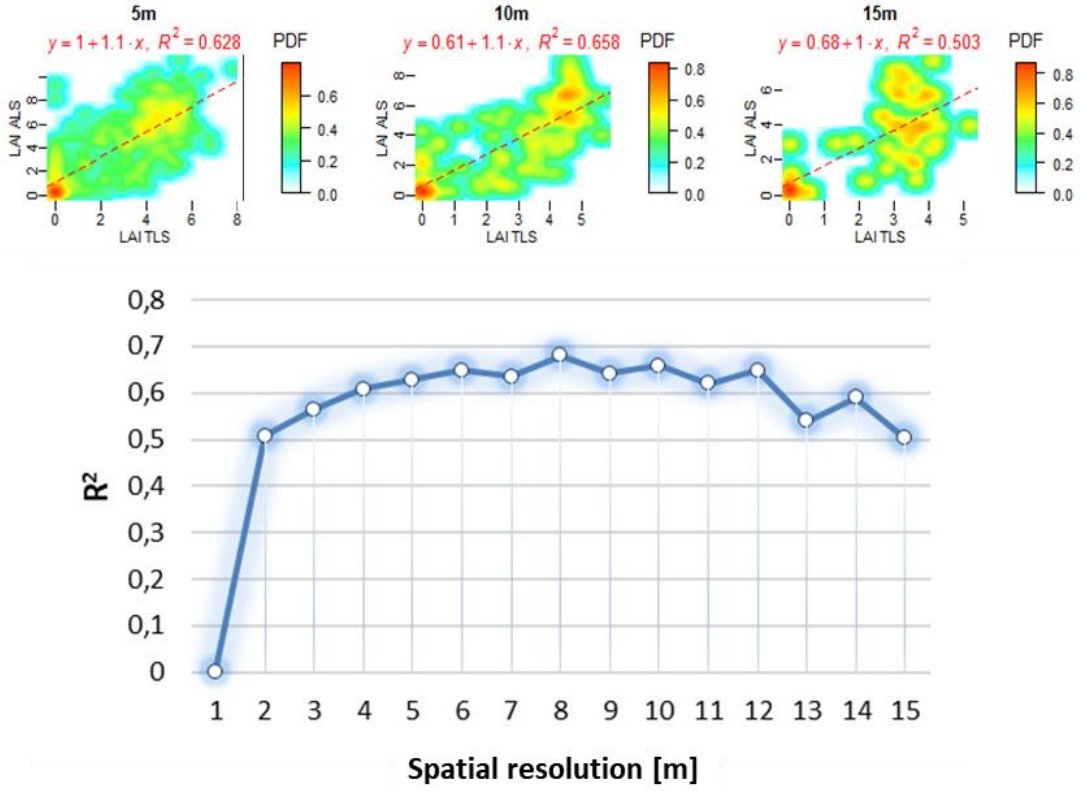

Figure 19. LAI_e per different cell sizes from TLS data and ALS data for the site of Moyzesova street. Data acquisition: 14 September 2016.

Conclusions

The presented report provide the following findings by analysing relation of the selected vegetation metrics derived from lidar datasets and Sentinel 2A imagery:

- NDVI correlated with more complex indices and it was decided to be sufficient for mapping the vegetation by Sentinel 2A.
- Canopy cover and canopy density derived from TLS and ALS data had weak correlation with NDVI derived from Sentinel 2A data.
- High NDVI values of Sentinel 2 imagery were co-located with high values of canopy density and canopy cover and vice versa.
- LAIe based on TLS and ALS most closely correlated with NDVI derived from Sentinel 2A data. This correlation was strong in the vegetation season and lower off this season.

The results opened more issues and questions to address than were answered. One of the most important is whether and how the response of the defined linear models can be improved and if a more suitable set of vegetation metric can be identified for relating the information of Sentinel 2 with 3D geometry. The reliability of the prediction of the vegetation transmittance from the Sentinel 2 data based on the reported findings will be tested in the following steps within the contract under WP3, which concerns developing the algorithmic structure for solar radiation modelling with implementation of vegetation transmittance under WP3.

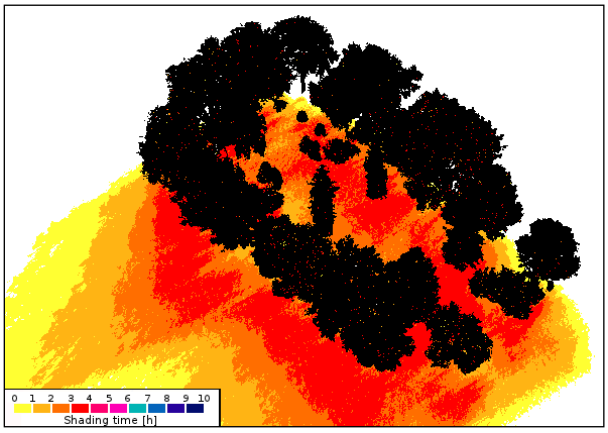

March

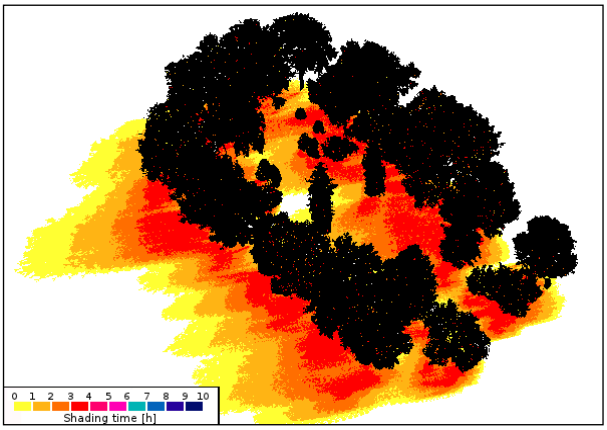

June

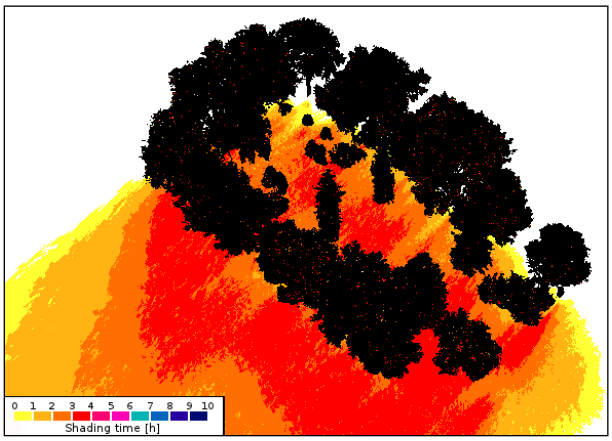

November

Figure 20. Simulation of time the area is shadowed by trees between 1 p.m. to 4 p.m. using the 3-D meshed tree models in the Shadow Analysis plugin of the SketchUp software for March, June and November. (adopted from Hofierka et al., 2017)

References

Alonzo, M., Bookhagen, B., McFadden, J.P., Sun, A., Roberts, D.A. (2015). Mapping urban forest leaf area index with airborne lidar using penetration metrics and allometry. Remote Sens. Environ., 162, pp. 141-153.

Campbell, J.B., Wynne, R.H., (2011). Introduction to Remote Sensing. 5th Edition, The Guilford Press.

Henrich, V., Krauss, G., Götze, C., Sandow, C. (2012): IDB - www.indexdatabase.de, Entwicklung einer Datenbank für Fernerkundungsindizes. AK Fernerkundung, Bochum, 4.-5. 10. 2012.

Hofierka, J., Gallay, M., Kaňuk, J., Šupinský, J. & Šašak, J., 2017. High-resolution urban greenery mapping for micro-climate modelling based on 3D city models. The International Archives of the Photogrammetry, Remote Sensing and Spatial Information Sciences (ISPRS Archives), XLII-4/W7, pp. 7-12.

Huete, A.R. (1988). A soil-adjusted vegetation index (savi). Remote Sens. Environ, 25, 295–309.

Jiang, Z.; Huete, A.R.; Didan, K.; Miura, T. (2008). Development of a two-band enhanced vegetation index without a blue band. Remote Sens. Environ., 112, 3833–3845

Jensen, J.R., (2006). Remote Sensing of the Environment: An Earth Resource Perspective. 2nd edition. Pearson.

Klingberg, J., Konarska, J., Lindberg, F., Johansson, L., Thorsson, S. (2017). Mapping leaf area of urban greenery using aerial LiDAR and ground-based measurements in Gothenburg, Sweden. Urban Forestry and Urban Greening. 26 (2017). pp. 31-40.

Onačillová, K., Gallay, M. (2018). Spatio-temporal analysis of surface urban heat island based on LANDSAT ETM+ and OLI/TIRS imagery in the city of Košice, Slovakia. Carpathian Journal of Earth and Environmental Sciences, 13(2), 395 - 408.

Richardson, J.J., Moskal, L.M., Kim, S.H. (2009). Modeling approaches to estimate effective leaf area index from aerial discrete-return LIDAR. Agric. For. Meteorol., 149, pp. 1152-1160.

Tooke, T.R., Coops, N.C., Goodwin, N.R., Voogt, J.A. (2009). Extracting urban vegetation characteristics using spectral mixture analysis and decision tree classifications. Remote Sensing of Environment, 113(2), pp. 398-407.

Tooke, T.R., Coops, N.C. Christen, A., Gurtuna, O., Prévot, A., (2012). Integrated irradiance modelling in the urban environment based on remotely sensed data. Solar Energy, 86(10), pp. 2923-2934.